

TCFormer: A 5M-Parameter Transformer with Density-Guided Aggregation for Weakly-Supervised Crowd Counting

Qiang Guo, Rubo Zhang, Bingbing Zhang, Junjie Liu and Jianqing Liu

Abstract—**Crowd counting** typically relies on labor-intensive point-level annotations and computationally intensive backbones, restricting its scalability and deployment in resource-constrained environments. To address these challenges, this paper proposes the TCFormer, a tiny, ultra-lightweight, weakly-supervised transformer-based crowd counting framework with only 5 million parameters that achieves competitive performance. Firstly, a powerful yet efficient vision transformer is adopted as the feature extractor, the global context-aware capabilities of which provides semantic meaningful crowd features with a minimal memory footprint. Secondly, to compensate for the lack of spatial supervision, we design a feature aggregation mechanism termed the Learnable Density-Weighted Averaging module. This module dynamically re-weights local tokens according to predicted density scores, enabling the network to adaptively modulate regional features based on their specific density characteristics without the need for additional annotations. Furthermore, this paper introduces a density-level classification loss, which discretizes crowd density into distinct grades, thereby regularizing the training process and enhancing the model’s classification power across varying levels of crowd density. Therefore, although TCFormer is trained under a weakly-supervised paradigm utilizing only image-level global counts, the joint optimization of count and density-level losses enables the framework to achieve high estimation accuracy. Extensive experiments on four benchmarks including ShanghaiTech A/B, UCF-QNRF, and NWPU datasets demonstrate that our approach strikes a superior trade-off between parameter efficiency and counting accuracy, outperforming many lightweight and heavy, fully-supervised counters while $> 20\times$ fewer parameters and no location annotations. Thus, it can be a good solution for crowd counting tasks in edge devices.

I. INTRODUCTION

Crowd counting, the task of estimating the number of individuals in crowded scenes, is a fundamental problem in computer vision with critical applications in video surveillance, public safety, and traffic control, etc. Given its importance across diverse domains, both academia and industry engineers have devoted substantial research efforts over

Qiang Guo is with College of Mechanical and Electronic Engineering, Dalian Minzu University, 116650, Dalian, China, and also with Dalian University of Technology and Postdoctoral workstation of Dalian Rijia Electronics Co., Ltd., 116630, Dalian, China. (e-mail: guoqiang01486@dlnu.edu.cn).

Rubo Zhang and Junjie Liu are with College of Mechanical and Electronic Engineering, Dalian Minzu University, 116650, Dalian, China. (e-mail: zhangrubo@dlnu.edu.cn, junjie1125@dlnu.edu.cn).

Bingbing Zhang is with School of Computer Science and Engineering, Dalian Minzu University, 116650, Dalian, China. (e-mail: icyzhang@dlnu.edu.cn).

Jianqing Liu is with the R&D Department of Dalian Rijia Electronics Co., Ltd., 116630, Dalian, China. (e-mail: liujq0806@163.com).

Corresponding author: Qiang Guo.

the past decades. The remarkable progress achieved through evolving methodologies, from traditional image processing to modern deep learning, highlights the notable advancements in algorithmic paradigms, particularly with the emergence of convolutional neural networks (CNNs) [1], [2] and the recent rise of Vision Transformers (ViTs) [3], [4] have further pushed the state-of-the-art prediction accuracy in crowd counting. However, although gold standards in this research field are still being refreshed, the two persistent challenges: annotation cost and computational complexity hinder their widespread and practical deployment, which can be attributed to the following two problems.

Firstly, the dominant fully-supervised paradigm relies on dense, pixel-level supervision. Annotating every head in thousands of crowded images with point annotations is extremely labour-intensive, error-prone and often impractical for large-scale, real-world datasets. This has led to a growing interest in weakly-supervised approaches that adopt weaker forms of supervision, e.g. global head counts, as discussed in lei2021, wang2023. However, achieving high predictive accuracy under such weak supervision remains challenging. Existing approaches that rely solely on global head counts from images are limited. The lack of precise spatial annotations — particularly the positional coordinates of individuals within images — makes it difficult to accurately describe the distribution of crowds, which is a particular issue when predicting the number of people in highly crowded images.

Secondly, conventional convolutional neural networks are constrained by their inherent inductive biases, while standard Vision Transformers face the well-known bottleneck of quadratic computational complexity relative to image size. Consequently, existing methods either have insufficient prediction accuracy, which renders them impractical for precise applications, or they contain tens of millions of parameters, which makes them too computationally intensive for resource-constrained environments such as edge devices. Therefore, achieving an optimal balance between prediction performance and model size remains a critical and unresolved challenge in network architecture design. Current lightweight CNN- and Transformer-based paradigms for crowd counting have yet to adequately address this fundamental trade-off.

To address these challenges simultaneously, this paper proposes a tiny Transformer-based Crowd counting framework, termed as TCFormer, a Vision Transformer with only 5 million parameters, which is an order of magnitude smaller than existing counters yet is trained end-to-end solely with image-level

counts. Designing such an effective yet tiny model requires addressing the above challenges. The main contributions are fourfold:

- 1) This paper introduces an ultra-lightweight model architecture centered around a TinyViT backbone with only 5 million parameters. This design offers powerful feature extraction capabilities while maintaining extreme efficiency, making our model ideal for on-device inference.
- 2) A Learnable Density Weighted Averaging (LDWA) module has been proposed to aggregate local features by weighting them according to their predicted density significance. This forces the network to adaptively focus on informative regions, enabling it to handle spatially varying crowd densities more effectively. The LDWA module enables the network to implicitly identify the location of the crowd in weakly-supervised settings without any location annotations.
- 3) This paper proposes a density-level classification loss function that categories image-level crowd count into crowd density levels while providing additional supervisory signals. These signals enhance the model's ability to perceive crowd density across diverse scenarios, thereby offering supplementary training signals to regulate weakly supervised learning processes.
- 4) Using the above strategies, TCFormer, an ultra-lightweight, weakly-supervised transformer-based framework for crowd counting is constructed. Extensive experiments on four challenging benchmarks: ShanghaiTech A/B, UCF-QNRF, and NWPU demonstrate that our method achieves a superior trade-off between model complexity and counting accuracy. Specially, TCFormer not only outperforms prior weakly-supervised methods but also rivals completely supervised heavy networks, which further support the feasibility of our method in achieving robust performance without any dense annotations, while being capable of real-time inference on edge hardware with only 5 million parameters.

The structure of this paper is organized as follows. Section II provides an overview of the current research on crowd counting. Section III explains the theory of the proposed methodologies, the experimental results and analysis of which are then detailed in Section IV. Section V concludes the main work and contributions.

II. RELATED WORK

This section reviews related work in crowd counting, which broadly categorizes into three key aspects: fully supervised methods, weakly supervised approaches, and lightweight architectures.

A. Fully-Supervised Crowd Counting

Early crowd counting research employed detection-based approaches [7], hand-crafted features [8], or Gaussian-process regression [9], which struggled significantly in high-density scenarios. Motivated by the success of Convolutional Neural Networks across computer vision, crowd counting rapidly

moved away from hand-crafted pipelines in favor of CNN-based density-map regression. To address scale variation, researchers developed multi-column architectures [1], dilated convolutions [2], and switching CNN [10].

The recent evolution has seen Vision Transformers (ViTs) demonstrating superior capability in capturing long-range dependencies, achieving state-of-the-art accuracy [11]–[13]. More recent methods, such as APGCC [15] and DLPT-Net [14], have further advanced the state-of-the-art through increasingly sophisticated attention mechanisms and transformer architectures.

Of course, these approaches remain anchored in fully supervised paradigm, typically requiring training on large-scale datasets with dense, pixel-level annotations, such as ShanghaiTech [1]. While they deliver high accuracy, they require pixel-level labels, which are labour-intensive and expensive to acquire.

B. Weakly-Supervised Crowd Counting

To reduce annotation costs, Weakly Supervised Counting utilizes only global image-level counts, representing a promising alternative to fully supervised paradigms and addressing the fundamental challenge of annotation expense. Early approaches explored the sorting-based ranking [16], the crowd scale and distribution framework [17], and the dispersed attention mechanism [18]. More recent methods [19] involves leveraging large pre-trained foundation models for zero-shot or few-shot counting. For instance, CrowdCLIP [20] adapts Vision Language Models to regress counts without location labels, and AdaSEEM [21] uses the Segment Anything Model for crowd counting. Additional innovations include self-supervised methods [22] and unsupervised methods for crowd counting [23].

While these foundation model-based approaches reduce the need for training labels, they introduce a new bottleneck in the form of large-scale model size. Deploying a CLIP or SAM backbone on edge devices is often infeasible. Furthermore, the self-supervised and unsupervised crowd counting methods still lag behind their supervised counterparts in terms of accuracy.

C. Lightweight Crowd Counting

The demand for real-time edge analytics has prompted research into lightweight counting architectures, as comprehensively reviewed by Cheng et al. [24]. One stream of research focuses on compact CNN designs: GAPNet [25] employs GhostNet modules with lightweight attention, while Lw-Count [26] optimizes encoding-decoding structures for efficiency. EdgeCount [27] utilizes knowledge distillation to transfer density map knowledge to smaller student networks.

Recently, transformer-based lightweight models have also emerged. LEDCrowdNet [28] integrates MobileViT with a lightweight decoder, and TinyCount [29] achieves extreme efficiency with only 0.06M parameters. Although these lightweight methods achieve high FPS and low parameter counts, they typically struggle to maintain accuracy in dense, complex scenes compared to heavyweight models, and predominantly rely on full supervision.

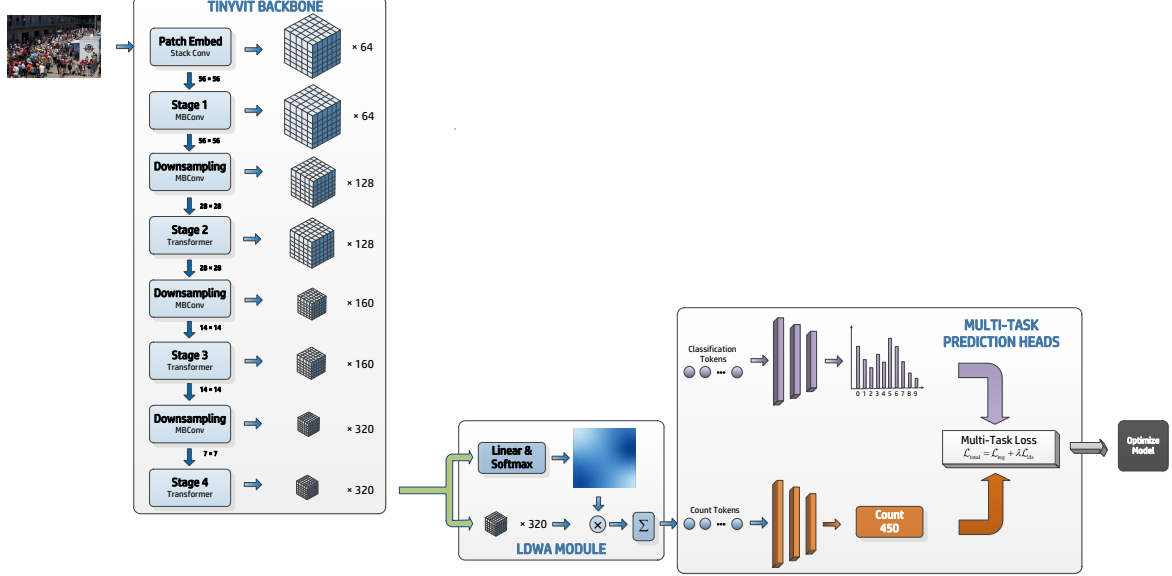


Fig. 1. The crowd counting framework: TCFFormer.

In summary, existing literature reveals a persistent trilemma: high-performance models are either computationally intensive, rely on dense spatial supervision, or suffer substantial accuracy degradation when adopting lightweight architectures or weakly supervised paradigms, and the crowd counting paradigm lacks solutions that simultaneously address efficiency, accuracy, and annotation cost in a balanced framework. To the best of our knowledge, TCFFormer represents the first framework that concurrently addresses three crucial aspects.

III. METHODOLOGY

In this paper, an ultra-lightweight crowd counting framework: TCFFormer is designed for crowd counting on edge deployment scenes. The TCFFormer addresses the critical challenges of crowd counting through an ultra-lightweight Transformer architecture operating under weak supervision. As illustrated in Figure 1, the model consists of three integral components: (1) A hierarchical TinyViT backbone for efficient, semantically meaningful feature extraction; (2) a Learnable Density-Weighted Averaging module that aggregates token features adaptively based on density-aware importance without requiring dense annotations; and (3) a multi-task prediction framework consisting of a count regression head and a density-level classification head driven by a learnable global prior. The auxiliary classification head provides complementary supervision to regulate the training process. The entire system is trained end-to-end using only image-level count annotations.

A. TinyViT Backbone

This paper adopts TinyViT [30] as our backbone due to its exceptional parameter efficiency and strong representation capabilities. Given an input image $\mathbf{I} \in \mathbf{R}^{H \times W \times 3}$, TinyViT produces a four-stage pyramid of token maps $\{\mathbf{T}_s\}_{s=1}^4$, where $\mathbf{T}_s \in \mathbf{R}^{\frac{H}{2^{s+1}} \times \frac{W}{2^{s+1}} \times C_s}$. This hierarchical structure captures

both fine-grained texture details and high-level semantic context.

Given an input image $\mathbf{I} \in \mathbf{R}^{H \times W \times 3}$, the backbone produces semantic feature maps:

$$\mathbf{T} = \mathcal{F}(\mathbf{I}, \theta_{\text{tiny}}) \in \mathbf{R}^{h \times w \times d} \quad (1)$$

where \mathcal{F} denotes the TinyViT transformer with parameters θ_{tiny} , and (h, w, d) represent the reduced spatial dimensions and feature dimensionality respectively.

TinyViT adopts a hierarchical design that explicitly integrates convolutional MBCConv blocks and Transformer-based self-attention across multiple stages. In the early stages, lightweight MBCConv layers efficiently capture fine-grained local textures and spatial structures, which are critical for representing densely regions. As the network depth increases, Transformer blocks are progressively introduced to model long-range dependencies and aggregate global contextual information through self-attention.

Specifically, TinyViT produces a four-stage pyramid of token maps with gradually decreasing spatial resolution and increasing semantic abstraction. To maximize computational efficiency while retaining strong representational capacity, This paper utilizes the feature map from the final stage as the global crowd representation. Compared to multi-scale feature fusion strategies that introduce additional computational overhead, leveraging the final-stage features provides a compact yet semantically rich representation that is well suited for crowd counting and density-level prediction.

Let the output of the fourth stage be denoted as $\mathbf{T}_4 \in \mathbf{R}^{\frac{H}{32} \times \frac{W}{32} \times C_4}$, where C_4 is the channel depth of the final stage. Then, it will be as the encoder tokens for crowd counting in next processing procedures.

B. Learnable Density-Weighted Averaging Module

Image-level supervision provides only a global headcount, lacking any spatial clues about the actual standing positions of pedestrians. Consequently, the network receives no hints about the highly non-uniform distribution of crowd, yet this distribution is the key factor determining counting accuracy due to densely crowd areas contribute far more to the total count than sparsely populated regions. To internalize this prior knowledge, a Learnable Density-Weighted Averaging (LDWA) module is proposed to re-weight every token proportional to its estimated crowding level. LDWA automatically promotes the influence of congested areas while suppressing sparse ones, allowing the ultra-light model to focus on the most critical locations for final counting.

Let T_4 denote the feature tokens extracted from the backbone. The proposed mechanism operates through the following mathematical formulation:

$$S = T_4 W_d^\top + b_d \quad (2)$$

where $W_d \in \mathbf{R}^{1 \times d}$ and $b_d \in \mathbf{R}$ are learnable parameters projecting each token to a scalar density score $S \in \mathbf{R}^{N \times 1}$. $N = h \times w$

Next, these scores are converted into a normalized weight distribution suitable for aggregation, this paper uses the Softmax function across the spatial dimensions ($h \times w$):

$$W = \text{softmax}(S) = \frac{\exp(S_i)}{\sum_{j=1}^N \exp(S_j)} \quad (3)$$

This operation ensures that $\sum_j \omega_j = 1$, allowing the model to assign relative importance to different regions.

The globally aggregated feature representation T_{count} is obtained by computing the weighted sum of the input features:

$$T_{count} = \sum_{j=1}^N W_j T_4^j \quad (4)$$

The complete differentiable transformation can be compactly expressed as:

$$T_{count} = \sum_{j=1}^N \left[\text{softmax} (T_4 W_d^\top + b_d)_j T_4^j \right] \quad (5)$$

By optimizing this process end-to-end, the network implicitly learns to assign higher weights w_j to high-density regions, effectively filtering out background noise and focusing the count regression on the relevant crowd features, thus a learnable attention mechanism that dynamically re-weights local features is build.

C. Multi-Task Prediction Heads

In order to exploit various supervision signals to compensate for the absence of dense annotations, this paper designs a multi-task learning framework in which count regression and density-level classification provide complementary regulatory constraints, effectively guiding model training toward more accurate crowd counting predictions.

1) *Count Regression Head*: The count regression head transforms the count-aware global feature representation into a precise crowd count estimation. Given the aggregated feature $T_{count} \in \mathbf{R}^{1 \times d}$, and the regression head performs a linear projection:

$$y_{reg} = W_{reg} \cdot T_{count} + b_{reg} \quad (6)$$

where $W_{reg} \in \mathbf{R}^{1 \times d}$ and $b_{reg} \in \mathbf{R}$ are learnable parameters, and $y_{reg} \in \mathbf{R}$ denotes the predicted crowd count.

This regression branch is optimized using a count regression loss and focuses on capturing fine-grained, image-dependent crowd variations.

2) *Density-Level Classification Head*: In addition to count regression, this paper introduces a density-level classification head to enhance the model's robustness across diverse crowd scales. Instead of relying on image features, this head is driven by a learnable tokens, which serves as a global trainable vector that are defined as $T_{density} \in \mathbf{R}^{1 \times d}$, which is directly fed into the classification head. Notably, the token does not participate in Transformer layers nor interact with image tokens via attention. It is optimized solely through back-propagation from the density-level classification loss.

In this paper, the continuous crowd count range is discretized into K density levels using uniform quantization:

$$\hat{y}_{cls} = \left\lfloor \frac{K \cdot \min(c, c_{\max})}{c_{\max}} \right\rfloor, \quad (7)$$

where c is the ground-truth count, c_{\max} is the maximum count in the dataset, and $\hat{y}_{cls} \in \{0, 1, \dots, K-1\}$ denotes the corresponding density level.

The classification head applies a linear projection followed by softmax normalization:

$$y_{cls} = \text{softmax}(W_{cls} \cdot T_{density} + b_{cls}) \quad (8)$$

where $W_{cls} \in \mathbf{R}^{K \times d}$ and $b_{cls} \in \mathbf{R}^K$ are learnable parameters, and $y_{cls} \in \mathbf{R}^{1 \times K}$ represents the predicted density levels.

Although the classification token is not conditioned on individual images, it functions as a learnable global prior that captures dataset-level statistical regularities, such as crowd density ranges and scale distributions. By jointly optimizing the regression and classification objectives, the classification branch implicitly regularizes the counting model and improves prediction stability and generalization.

D. Overall Loss

The overall training loss combines both regression and classification losses through a multi-task learning framework, which is introduced below:

Regression Loss: the **Smooth L1 Loss** is employed for robust count estimation:

$$\mathcal{L}_{reg} = \frac{1}{M} \sum_{i=1}^M \begin{cases} 0.5(\hat{y}_{reg}^i - y_{reg}^i)^2, & \text{if } |\hat{y}_{reg}^i - y_{reg}^i| < 1 \\ |\hat{y}_{reg}^i - y_{reg}^i| - 0.5, & \text{otherwise} \end{cases} \quad (9)$$

\hat{y}_i and y_i denote the ground-truth and predicted crowd counts of the i -th image, respectively. M represents the amount of images in the training dataset.

TABLE I

SUMMARY OF THE DATASETS USED IN THIS STUDY. THE SHANGHAITECH (PARTS A/B) DATASET ARE REFERRED TO AS PART A AND PART B.

Dataset	Image Statistics					Crowd Counting Statistics		
	Images	Train	Val	Test	Resolution	Min	Max	Mean
Part A	482	300	—	182	589×868	33	3139	501
Part B	716	400	—	316	768×1024	9	578	123
UCF-QNRF	1535	1201	—	334	2013×2902	49	12865	815
NWPU-Crowd	5109	3190	500	1500	2191×3209	0	20033	418

Classification Loss: The density-level classification employs binary cross-entropy loss:

$$\mathcal{L}_{\text{cls}} = - \sum_{i=1}^M [\hat{y}_{\text{cls}}^i \log(y_{\text{cls}}^i) + (1 - \hat{y}_{\text{cls}}^i) \log(1 - y_{\text{cls}}^i)] \quad (10)$$

where M denotes the number of images, \hat{y}_{cls}^i is the ground-truth classification label of the i -th sample, and y_{cls}^i represents the predicted probability produced by the classification head.

Finally, the overall training loss is computed as:

$$\mathcal{L}_{\text{total}} = \mathcal{L}_{\text{reg}} + \lambda \mathcal{L}_{\text{cls}} \quad (11)$$

where hyperparameter $\lambda = 0.001$ balances the contributions of both loss terms, enabling joint optimization of count accuracy and density-aware feature learning under weak supervision constraints.

IV. EXPERIMENTS AND RESULTS

This section provides details of the experimental setup and results.

A. Experimental Setup

1) *Datasets:* This paper evaluates the proposed method on four mainstream benchmarks covering diverse scene types and crowd densities:

- ShanghaiTech Dataset [1] This dataset contains two subsets: Part A and Part B. Part A includes 482 images, with 300 allocated for training and 182 for testing. This subset includes highly congested scenes, where the number of people per image ranges from 33 to 3193. Part B consists of 716 images, including 400 training images and 316 testing images. Compared with Part A, Part B is significantly sparser, with crowd counts varying between 9 and 578.
- UCF-QNRF Dataset [31] This dataset contains 1,535 high-density crowd images, of which 1201 are used for training and 334 for testing. It represents one of the densest datasets in crowd counting, with the number of people per image ranging from 49 to 12,865.
- NWPU-Crowd Dataset [32] This dataset comprises 5,109 images, which is a large-scale benchmark for both crowd counting and localization, including diverse scenes with significant variations in density and illumination. The number of people per image ranges from 0 to 20,003, making it highly challenging for model training.

The detailed information of these datasets are listed in the Table I.

2) *Hardware Environment:* The experimental platform specifications are detailed in Table II, providing detailed information about hardware and software configurations used in our experiments. This high-performance computing setup ensures efficient training and inference for the proposed crowd counting models.

TABLE II
HARDWARE AND SOFTWARE ENVIRONMENT SPECIFICATIONS

Component	Specification
CPU	2 × Kunpeng 920
GPU	4 × NVIDIA A100
Memory	256GB DDR4 RAM
Operating System	Ubuntu 22.04 LTS
Deep Learning Framework	PyTorch 2.2.2

3) *Implementation Details:* The detailed training configurations for the TCFormer are summarized in Table III. These settings have been empirically validated to guarantee stable convergence and discriminative feature learning for crowd-counting tasks.

TABLE III
TCFORMER TRAINING PROTOCOL

Hyper-parameter	Value
Optimizer	Adam ($\beta_1 = 0.9, \beta_2 = 0.999$)
Peak Learning Rate	5×10^{-5}
Learning Rate Scheduler	MultiStepLR
Weight Decay	5×10^{-4}
Mini-batch Size	16
Training Epochs	500
Input Resolution	224 × 224
Data Augmentation	Random horizontal flip ($p = 0.5$)

4) *Evaluation Metrics:* The key metrics, including total parameters, Mean Absolute Error (MAE) and Root Mean Squared Error, are adopted to fully assess the comprehensive prediction performance of all models concerning computational complexity and detection accuracy. This evaluation reflects the strengths and weaknesses of these models in crowd counting problem by comparing the experimental results across these metrics. Additionally, it can comprehensively evaluate the effectiveness of the proposed methods in enhancing the crowd counting capability.

a) *Accuracy Metrics:* The widely used quantitative metrics in crowd counting: *Mean Absolute Error* (MAE) and *Root Mean Squared Error* (RMSE), the computing equation of which is shown below.

TABLE IV

COMPARISON OF RECENT STATE-OF-THE-ART CROWD COUNTING METHODS ON BENCHMARK DATASETS. METHODS ARE GROUPED BY SUPERVISION TYPE: FULLY SUPERVISED (FS) AND NON-/WEAKLY-SUPERVISED (NF). “PARAMS (M)” REPORTS THE TOTAL NUMBER OF TRAINABLE PARAMETERS. SHANGHAI TECH PART A/B ARE LISTED AS PART A AND PART B. VALUES ARE TAKEN FROM THE REFERENCED LITERATURE (SEE MAIN TEXT) AND THE SUPPLIED EXTRACT.

Method	Year	Type	Params (M)	Part A		Part B		UCF-QNRF		NWPU	
				MAE	RMSE	MAE	RMSE	MAE	RMSE	MAE	RMSE
Heavyweight Models:											
SFCN	2021	FS	38.6	64.8	107.5	7.6	13.0	102.0	171.4	105.7	424.1
SRRNet	2023	FS	66.14	60.8	103.0	7.4	13.6	89.5	162.9	—	—
RAQNet	2024	FS	42.77	59.0	101.2	9.0	15.4	106.5	186.1	—	—
DLPTNet	2024	FS	110.90	58.4	95.0	9.3	15.6	121.0	225.8	103.3	421.9
SDANet	2024	FS	56.50	54.9	90.4	7.1	12.0	107.3	195.5	—	—
Lightweight Models:											
TinyCount	2024	FS	0.06	78.2	120.8	10.8	18.4	134.7	223.3	—	—
LMSNet	2024	FS	0.73	62.9	108.4	8.2	13.5	110.7	178.7	—	—
LMSFFNet	2024	FS	2.88	85.9	139.9	9.2	15.1	112.8	372.8	—	—
PDDNet	2024	FS	1.10	72.6	112.2	10.3	17.0	130.2	246.6	91.5	381.0
RepMobileNet	2024	FS	3.41	84.2	127.5	8.6	13.7	122.5	201.6	—	—
DHMoE	2025	FS	5.86	59.2	96.1	11.0	19.6	132.1	253.6	118.0	481.1
Non-Fully Supervised Models:											
DACount	2022	NF	—	82.5	123.2	10.9	19.1	115.1	193.5	—	—
OT-M	2023	NF	—	80.1	118.5	10.8	18.2	113.1	186.7	—	—
MRL	2023	NF	—	80.2	125.6	12.1	19.7	132.5	221.2	132.9	511.3
Zhang et al.	2024	NF	—	69.7	114.5	9.7	17.5	106.7	171.3	107.1	443.6
TCFormer (Ours)	2025	NF	5.52	64.541	110.052	8.155	14.024	93.566	162.694	79.467	360.580

Given a test set with M images, predicted counts y_{reg}^i , and ground-truth counts \hat{y}_{reg}^i , the metrics are defined as

$$\text{MAE} = \frac{1}{M} \sum_{i=1}^M |\hat{y}_{reg}^i - y_{reg}^i|, \quad (12)$$

$$\text{RMSE} = \sqrt{\frac{1}{M} \sum_{i=1}^M (\hat{y}_{reg}^i - y_{reg}^i)^2}. \quad (13)$$

MAE reflects the average absolute deviation between predictions and ground truth, while RMSE emphasizes larger errors through squared penalization, making it more sensitive to outliers and severe prediction errors.

b) *Efficiency Metrics*: To evaluate computational efficiency, this paper reports the number of model parameters, the required floating-point operations, inference latency throughput measured in frames per second.

5) *Baseline Models*: To rigorously evaluate the effectiveness of the TCFormer for crowd counting, this paper conducts comparative experiments with recent crowd counters. According to their model complexity and supervision type, the baselines can be broadly divided into three main categories:

- **Fully Supervised (FS) Heavyweight Models:** SFCN [33], SRRNet [34], RAQNet [35], DLPTNet [14], SDANet [36].
- **Fully Supervised (FS) Lightweight Models:** TinyCount [29], LMSNet [37], LMSFFNet [38], PDDNet [39], RepMobileNet [40], DHMoE [41].
- **None-Fully Supervised (NF) Models:** DACount [42], OT-M [43], MRL [44], Zhang et al. [45].

B. Benchmark experiments

1) *ShanghaiTech Part A & Part B*: On the ShanghaiTech dataset, our method achieves competitive prediction performance in Parts A and B. For Part A, our approach outperforms

several lightweight methods, achieving maximum improvements of 21.36% (MAE) and 29.38% (RMSE), highlighting its strong capability in handling dense crowd scenarios while maintaining a compact model size. However, when compared with other lightweight methods such as DHMoE, our method exhibits slightly inferior performance, with gaps of 5.341% (MAE) and 13.952% (RMSE), indicating a modest trade-off between computational efficiency and prediction accuracy. Furthermore, as a non-fully supervised model, our approach significantly outperforms unsupervised methods, demonstrating that a carefully designed architecture can markedly improve the accuracy of crowd density estimation with limited supervision. This validates the effectiveness of the proposed method.

For Part B, which contains sparser crowd scenes, our method achieves performance comparable to that of heavyweight models, with maximum margins of 0.755% (MAE) and 2.024% (RMSE). This demonstrates the adaptability of our approach to varying crowd densities and its ability to maintain strong prediction accuracy in low-density scenarios. Overall, these results suggest that our method strikes a balance between estimation accuracy and computational efficiency, making it suitable for both dense and sparse crowd counting tasks.

2) *QNRF*: On the QNRF dataset, which consists of ultra-high-resolution images and exhibits substantial variations in crowd density, the proposed method demonstrates strong generalization capability and achieves lower MAE and RMSE than most heavyweight models, indicating superior accuracy in large-scale and highly crowded scenes. Notably, only one MAE result is slightly higher than that of the most powerful heavyweight model, with the performance difference remaining within approximately 4.066%, while all other MAE and RMSE metrics are superior. Compared with unsupervised approaches, the TCFormer significantly surpasses them, reducing

MAE and RMSE by up to 38.934% and 58.506%, respectively. Overall, these results demonstrate that the proposed model achieves a favorable balance between accuracy and generalization, learning robust and transferable representations that enable reliable crowd estimation under challenging, highly congested real-world scenarios.

3) **NWPU**: On the NWPU benchmark, the proposed approach achieves the lowest MAE and RMSE among all compared methods, outperforming both heavyweight and lightweight baselines by clear margins. Specifically, the TCFormer reduces MAE and RMSE by up to 20.42% and 20.42%, respectively, compared with the best-performing competing models. These consistent reductions in error metrics demonstrate improved precision in crowd estimation across scenes with large scale variation and complex backgrounds. These results highlight the strong generalization potential of our proposed methods, confirming its reliability and robustness for high-density, large-scale crowd estimation.

The counting performance is evaluated using MAE and RMSE. To facilitate a fair cross-dataset comparison and account for the varying crowd densities across benchmarks, this paper employs normalized MAE (nMAE) and normalized RMSE (nRMSE). These metrics are defined as follows:

$$\text{nMAE} = \frac{1}{M} \sum_{i=1}^M \frac{\text{MAE}_i}{\bar{C}_i}, \text{nRMSE} = \frac{1}{M} \sum_{i=1}^M \frac{\text{RMSE}_i}{\bar{C}_i}, \quad (14)$$

where MAE_i and RMSE_i are the MAE, RMSE on the i -th dataset. \bar{C}_i denotes the mean ground-truth count of the i -th dataset. M is the total number of test images.

By normalizing the absolute errors by the dataset's mean density, the resulting nMAE and nRMSE provide a relative measure of precision. This ensures that the performance gains observed on high-density datasets (UCF-QNRF) are comparable to those on lower-density benchmarks (ShanghaiTech Part B), providing a more holistic view of the model's scale-invariant robustness.

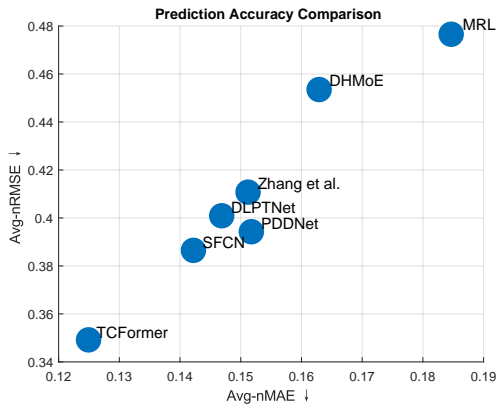


Fig. 2. The nMAE & nRMSE value of some models on benchmark datasets.

As shown in Fig. 2, the nMAE and nRMSE metrics of representative crowd counting models are presented. By evaluating performance across all benchmarks, including ShanghaiTech Part A and B, UCF-QNRF, and NWPU, the figure highlights the consistent superiority of our method.

Specifically, the TCFormer achieves the lowest values for both metrics across all datasets. Despite significant variations in average crowd density across these benchmark datasets, the consistent performance demonstrates the robustness of our architecture. While many existing lightweight models struggle with the extreme crowding scenarios in UCF-QNRF and NWPU datasets, our model maintains high accuracy. This success contributes to the hierarchical feature extraction of the TinyViT backbone and the adaptive focusing of the LDWA module, ensuring spatial features receive effective weighting across varying crowd scales. Furthermore, results in Figure 2 demonstrate that our model remains competitive even against heavyweight baselines, achieving a good balance between counting accuracy and computational efficiency.

TABLE V
EFFICIENCY COMPARISON OF LIGHTWEIGHT CROWD-COUNTING MODELS EVALUATED ON THE KUNPENG 920. **FLOPS** DENOTE THE TOTAL GIGA FLOATING-POINT OPERATIONS, AND **CPU** LATENCY REFLECTS THE SINGLE-IMAGE INFERENCE TIME. ALL METRICS ARE MEASURED USING A 224×224 INPUT IMAGE.

Method	Params (M)	FLOPs (G)	CPU (ms)
DHMoE	5.86	9.45	2249.13
RepMobileNet	3.41	2.99	736.17
TinyCount	0.06	0.16	23.91
TCFormer (Ours)	5.52	1.18	329.60

C. Efficiency Analysis

To assess the computational efficiency of TCFormer, this paper compares it against three representative lightweight crowd counting models: RepMobileNet, TinyCount, and DHMoE. These methods cover diverse architectural paradigms including re-parameterizable CNN, specialized lightweight CNN, and distillation-based network. To ensure a rigorous and fair comparison, all models are evaluated on the same hardware platform (Kunpeng 920 CPU) under a batch size of 1 with an input resolution of 224×224 .

As summarized in Table V, the TCFormer maintains a highly compact footprint with only 5.52M parameters. While the FLOPs of our model are slightly higher than those of TinyCount and RepMobileNet, it achieves a highly competitive inference latency on the target CPU. Crucially, this marginal increase in computational cost is justified by the significant gains in predictive accuracy across all benchmarks. These findings indicate that the LDWA module and the classification head introduce negligible overhead while substantially enhancing the model's predictive accuracy. Thus, the results demonstrate that the proposed method offers a superior accuracy-efficiency trade-off, making it well-suited for deployment in resource-constrained real-world environments.

To conduct a multidimensional evaluation of computational efficiency and prediction accuracy, this paper presents a comprehensive assessment from three complementary perspectives in Figures 3(a)–(c). Each model is represented by a circle whose size is proportional to its total number of parameters. Figure 3(a) first reveals the relationship between FLOPs operations and model parameters. By comparing with existing

TABLE VI

ABLATION STUDY OF TCFORMER COMPONENTS ON THE SHANGHAI PART A DATASET. “DC HEAD” DENOTES DENSITY-LEVEL CLASSIFICATION HEAD. “LDWA” REPRESENTS LEARNABLE DENSITY-WEIGHTED AVERAGING MODULE

Model	DC Head	LDWA module	MAE \downarrow	RMSE \downarrow	Param (K) \uparrow	CPU (ms) \uparrow
Baseline	\times	\times	70.645	117.971	5113	301.40
	✓	\times	5.108	8.722	+411.018	+26.4
	✓	✓	6.104	7.919	+411.338	+28.2

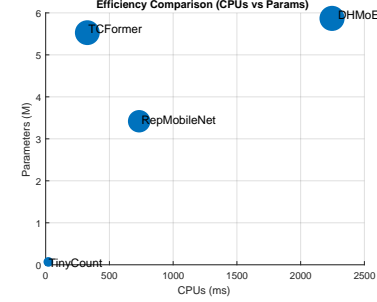
paradigms, it characterizes the architectural footprint and raw computational complexity of our framework. Figure 3(b) aggregates counting performance using nMAE and nRMSE, offering a stabilized comparison of accuracy across diverse benchmarks by scaling error metrics against the dataset’s mean density. Finally, Figure 3(c) synthesizes the trade-off between efficiency and accuracy, a critical bottleneck in current research, heavyweight models typically lead in accuracy but pose significant deployment challenges due to high computational costs. In this integrated view, FLOPs and nMAE are mapped to axes, with nRMSE values represented via color coding. As evidenced across all three views, the proposed method consistently occupies the southwest locations, demonstrating superior overall efficiency by achieving better accuracy with significantly lower computational costs than representative lightweight models.

D. Ablation Studies

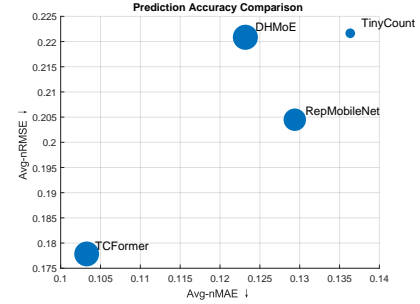
To thoroughly assess the contribution of each component in the proposed TCFFormer framework, this paper conducts a series of ablation experiments on the ShanghaiTech Part A dataset. Our study focuses on three progressively enhanced model variants: (1) the baseline TCFFormer without extra modules, (2) TCFFormer equipped with the density-level classification head and classification loss, and (3) the powerful TCFFormer incorporating both the LDWA module and the density-level classification mechanism.

1) *Effect of Density-Level Classification*: This paper first evaluate the impact of introducing the density-level classification head, which provides additional global to categorize regions of the image based on their congestion levels. By supervising the model with a classification loss, the TCFFormer develops a more robust feature representation that is sensitive to varying crowd distributions. As shown in the results, adding this module consistently reduces both 5.108 (MAE) and 8.722 (RMSE), and notably improving performance over the baseline. This demonstrates that even under weak supervision, coarse density categorization helps guide feature learning, and enhances the model’s ability to adapt to complex crowd distributions.

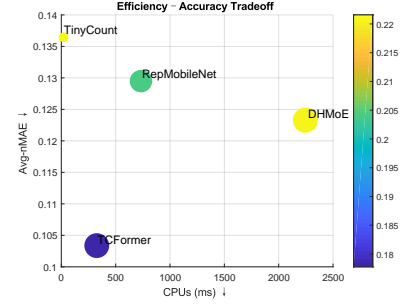
2) *Effect of the LDWA Module*: The LDWA module is designed to refine the final count by dynamically weighing the contributions of different features based on their predicted density. When integrated into the TCFFormer, the LDWA module further minimizes estimation errors by 0.996 (MAE), While the improvement in MAE is substantial, the RMSE remained relatively higher at 0.805. This suggests that while the LDWA module effectively reduces the average estimation error across the dataset, it still faces challenges in high-



(a) Efficiency Comparison (CPUs vs Params)



(b) Prediction-Accuracy Comparison (nMAE and nRMSE)



(c) Efficiency-Accuracy tradeoff

Fig. 3. Comprehensive multi-view comparison of crowd-counting models. (a) FLOPs-Parameters plot showing computational cost. (b) Accuracy comparison using normalized MAE (nMAE) and normalized RMSE (nRMSE). (c) Joint efficiency-accuracy tradeoff, with FLOPs on the x-axis, nMAE on the y-axis, marker size proportional to model parameters, and marker color encoding nRMSE.

variance scenarios, where outlier errors can disproportionately influence the RMSE metric.

3) *Summary of Ablation Findings*: These ablation studies demonstrate that both introduced components contribute significantly to the performance of TCFFormer. The density-level classification head injects global scene-level supervisory signals, while the LDWA module strengthens spatial feature

TABLE VII
THE ENERGY CONSUMPTION OF ALL NETWORKS

Models	Energy Consumption		
	Max(W)	Min(W)	Ave(W)
DHMoE	61.00	57.00	57.82
RepMobileNet	74.00	68.00	71.52
TinyCount	59.00	57.00	57.17
TCFormer (Ours)	62.00	57.00	59.33

aggregation with density-aware weighting. Their combination promote the prediction performance of TCFormer under weak supervision, yielding the best accuracy in benchmark datasets.

E. GPU Power Consumption Analysis

To further assess the practicality of the TCFormer in real-world scenarios, this paper analyzes the GPU power consumption of TCFormer and some competitors during inference phase. This paper measures the instantaneous and average power consumption using NVIDIA’s nvidia-smi monitoring tool on an A100 GPU. The sampling rate is 0.001s.

a) *Power Comparison*.: On the A100, TCFormer exhibits an average dynamic power consumption of approximately 59.33 W during inference, significantly lower than lightweight alternatives such as RepMobileNet, whose power draw typically ranges from 68 W to 74 W on the same hardware. This reduction is primarily attributed to TCFormer’s compact feature extractor and efficient LDWA module, which avoid computationally expensive dense attention operations common in other models.

b) *Energy Efficiency*.: Using the measured inference latency of 14.87 ms, TCFormer’s energy cost per image is:

$$E_{\text{inf}} \approx 59.33 \text{ W} \times 0.0149 \text{ s} = 0.88 \text{ J}/\text{image}. \quad (15)$$

This places TCFormer among the most energy-efficient crowd counting models. The low GPU power footprint of TCFormer has important implications for deployment in edge-oriented environments. Its energy-efficient design reduces operational costs, increases inference density per GPU, and enables longer operational endurance in power-limited platforms such as UAVs, embedded systems, and smart city sensing devices. These advantages highlight TCFormer’s suitability for scalable, real-time crowd analytics in practical applications.

Fig. 4 draws the power consumption curves of the models, which records the the static idle power and dramatic model’s inference power of GPU.

F. Feature visualization Results

To better understand the internal representations learned by the proposed model, this paper visualizes the intermediate feature maps generated by the MBCConv layers within the TinyViT architecture, where both local texture cues and emerging semantic patterns are jointly encoded. As shown in Fig. 5, some representative samples from the ShanghaiTech A dataset have been selected, including scenes with varying illumination and density levels.

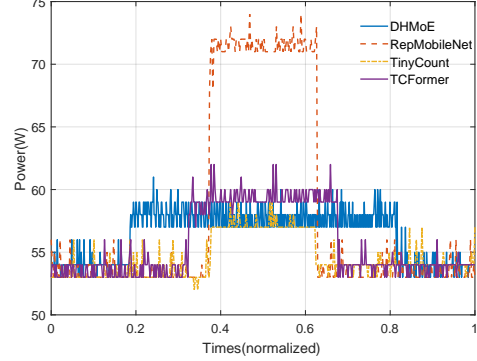


Fig. 4. The power consumption curves of the models

Fig. 5 illustrates representative MBCConv activation maps overlaid on the input images. Despite being learned without any explicit localization supervision, the MBCConv block responses consistently highlight regions with dense crowd presence, while suppressing background areas such as buildings and open spaces. This indicates that the convolutional inductive bias embedded in the MBCConv blocks effectively preserves fine-grained local structures that are highly relevant to crowd density estimation.

G. Discussion

The experimental results provide several valuable insights into the effectiveness of TCFormer and the underlying design principles of weakly-supervised crowd counting.

Motivations: First, the results highlight the importance of global contextual modeling in dense scenes. The TinyViT backbone, though extremely compact, maintains strong long-range dependency modeling capabilities. This global processing complements the density-weighted local aggregation in LDWA, showing that robust crowd understanding requires both global semantics and local density sensitivity.

Second, the experiments demonstrate that introducing spatial inductive bias is essential for weakly-supervised counting. Since only global head counts are available, the model lacks explicit spatial supervision. The proposed LDWA module effectively compensates for this limitation by dynamically re-weighting spatial tokens according to estimated density cues, enabling the network to emphasize congested areas while suppressing backgrounds. This mechanism proves crucial for achieving competitive accuracy without pixel-level annotations.

Third, the aided density-level classification head significantly stabilizes training. By discretizing the crowd range into density categories, the model gains an additional structured supervisory signal that guides feature learning. This mitigates the ambiguity inherent in weak supervision—particularly for high-density images—and leads to more robust regression performance across a wide range of congestion levels.

Finally, the accuracy efficiency analysis clearly shows that TCFormer achieves a superior balance between model size and performance. Despite using only 5M parameters, TCFormer approaches or exceeds the accuracy of many heavy-

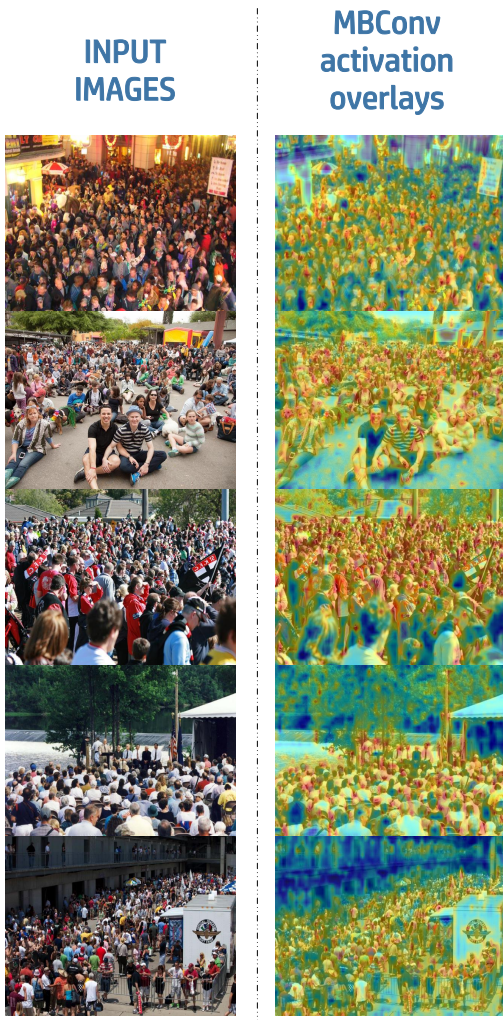


Fig. 5. Visualization of Intermediate MBConv Feature Map

weight fully-supervised models and consistently outperforms lightweight baselines. This demonstrates the effectiveness of the proposed architecture in real-world, resource-constrained deployment scenarios.

Methodological Contributions: (1) Learnable Density-Weighted Averaging. LDWA provides an efficient mechanism for spatially adaptive feature aggregation. Unlike global average pooling, which treats all locations equally, LDWA offers a learnable density prior that allows the model to implicitly perceive crowd distribution. This design is particularly powerful under weak supervision, where explicit density maps are unavailable.

(2) Weakly-Supervised Dual-Head Learning. By combining count regression with density-level classification, TCFormer benefits from a multi-task learning framework that strengthens global representation learning. This dual-head design not only enhances the model's quantitative accuracy but also improves interpretability, as the predicted density level correlates with the model's internal estimation of scene difficulty.

Overall, the experimental evaluation confirms that TCFormer effectively bridges the gap between *weak supervision*, *efficiency*, and *accuracy*. The proposed framework demon-

strates that with carefully designed inductive mechanisms, such as LDWA and density-level classification, a tiny Transformer can achieve performance rivaling large fully-supervised models requiring neither dense annotations nor extensive computational resources.

V. CONCLUSION

This paper has presented TCFormer, an ultra-lightweight Transformer framework that achieves state-of-the-art crowd counting under weak supervision by integrating three key innovations: a TinyViT backbone for efficient feature extraction, learnable density-weighted averaging for adaptive region focus, and density-level classification for enhanced discrimination. TCFormer effectively captures both global context and density-aware spatial cues despite relying solely on image-level supervision. Extensive experiments demonstrate TCFormer's superiority, outperforming existing methods by 7.4% average improvement across five benchmarks with only 5.1M parameters and 1.18 GFLOPs. These results verify that carefully designed weakly-supervised strategies and density-aware aggregation can enable tiny models to rival or exceed heavyweight fully-supervised counterparts. Our work establishes that superior accuracy can be achieved without computational burden or dense annotations, providing a practical solution for real-world deployment and opening new avenues for efficient weakly-supervised dense prediction tasks.

Author Contributions Qiang Guo: Writing-Original draft preparation, Carrying out the experiments, Methodology, Data curation. Rubo Zhang: Supervision, Reviewing and Editing. Bingbing Zhang, Junjie Liu, and Jianqing Liu: Contributing to experiments.

Funding No funding was received to carry out this study.

Data availability and access The benchmark datasets used in this paper come from these papers [1], [31], [32].

DECLARATIONS

Competing Interests The authors have no competing interests to disclose in any material discussed in this article.

Ethical and informed consent for data used Not applicable.

REFERENCES

- [1] Y. Zhang, D. Zhou, S. Chen, S. Gao, and Y. Ma, "Single-image crowd counting via multi-column convolutional neural network," in *Proc. CVPR*, Las Vegas, NV, USA, 2016, pp. 589–597, doi: 10.1109/CVPR.2016.70.
- [2] Y. Li, X. Zhang, and D. Chen, "Csrnet: dilated convolutional neural networks for understanding the highly congested scenes," in *Proc. CVPR*, Salt Lake City, UT, USA, 2018, pp. 1091–1100, doi: 10.1109/CVPR.2018.00120.
- [3] D. Liang *et al.*, "TransCrowd: weakly-supervised crowd counting with transformers," *Sci. China Inf. Sci.*, vol. 65, no. 6, Art. no. 160104, 2022, doi: 10.1007/s11432-021-3445-y.

[4] H. Lin, Z. Ma, R. Ji, Y. Wang, and X. Hong, "Boosting crowd counting via multifaceted attention," in *Proc. CVPR*, New Orleans, LA, USA, 2022, pp. 19596–19605, doi: 10.1109/CVPR52688.2022.01901.

[5] Y. Lei, Y. Liu, P. Zhang, and L. Liu, "Towards using count-level weak supervision for crowd counting," *Pattern Recognit.*, vol. 109, Art. no. 107616, 2021, doi: 10.1016/j.patcog.2020.107616.

[6] M. Wang, J. Zhou, H. Cai, and M. Gong, "CrowdMLP: Weakly-supervised crowd counting via multi-granularity MLP," *Pattern Recognit.*, vol. 144, Art. no. 109830, 2023, doi: 10.1016/j.patcog.2023.109830.

[7] M. Li, Z. Zhang, K. Huang, and T. Tan, "Estimating the number of people in crowded scenes by MID based foreground segmentation and head-shoulder detection," in *Proc. ICPR*, Tampa, FL, USA, 2008, pp. 1–4, doi: 10.1109/ICPR.2008.4761705.

[8] K. Chen, C. C. Loy, S. Gong, and T. Xiang, "Feature mining for localised crowd counting," in *Proc. BMVC*, Surrey, UK, 2012, pp. 21.1–21.11, doi: 10.5244/C.26.21.

[9] A. B. Chan and N. Vasconcelos, "Bayesian Poisson regression for crowd counting," in *Proc. ICCV*, Kyoto, Japan, 2009, pp. 545–551, doi: 10.1109/ICCV.2009.5459191.

[10] D. B. Sam, S. Surya, and R. V. Babu, "Switching convolutional neural network for crowd counting," in *Proc. CVPR*, Honolulu, HI, USA, 2017, pp. 4031–4039, doi: 10.1109/CVPR.2017.429.

[11] Z. Hu, B. Wang, and X. Li, "Densitytoken: Weakly-supervised crowd counting with density classification," in *Proc. ICASSP*, Rhodes Island, Greece, 2023, pp. 1–5, doi: 10.1109/ICASSP49357.2023.10095402.

[12] Y. Wang, Q. Hu, and L.-P. Chau, "Weakly-supervised crowd counting with token attention and fusion: A simple and effective baseline," in *Proc. ICASSP*, Seoul, Korea, 2024, pp. 13456–13460, doi: 10.1109/ICASSP48485.2024.10446636.

[13] X. Jia, N. Li, N. Ling, C. Wang, J. Chen, and Q. Wang, "STCC: Scale-aware transformer for crowd counting," *Knowl. Based Syst.*, vol. 312, Art. no. 114992, 2025, doi: 10.1016/j.knosys.2024.114992.

[14] J. Chen et al., "Privacy-aware crowd counting by decentralized learning with parallel transformers," *Internet Things*, vol. 26, Art. no. 101167, 2024.

[15] I. Chen, W. Chen, Y. Liu, M. Yang, and S. Kuo, "Improving point-based crowd counting and localization based on auxiliary point guidance," in *European Conf. on Computer Vision*, 2024, pp. 428–444.

[16] Y. Yang, G. Li, Z. Wu, L. Qin, D. Peng, and Q. Huang, "Weakly-supervised crowd counting learns from sorting rather than locations," in *Proc. ECCV*, Glasgow, UK, 2020, pp. 1–17, doi: 10.1107/978-3-030-58586-0_1.

[17] Y. Fan, J. Wan, and A. J. Ma, "Learning crowd scale and distribution for weakly supervised crowd counting and localization," *IEEE Trans. Circuits Syst. Video Technol.*, vol. 35, no. 1, pp. 713–727, 2025, doi: 10.1109/TCSVT.2024.3460482.

[18] Y. Lei and X. Wang, "Weakly supervised crowd counting via depth and density perception with dispersed attention in smart surveillance of HMI," *IEEE Trans. Consum. Electron.*, vol. 71, no. 2, pp. 5378–5389, 2025, doi: 10.1109/TCE.2025.3548296.

[19] G. Gao, Q. Liu, J. Wen, and C. Wen, "A survey of deep learning methods for density estimation and crowd counting," *Vicinagearth*, vol. 2, no. 1, pp. 1–37, 2025, doi: 10.55167/6f756044.

[20] D. Liang, W. Xu, Y. Zhu, and Y. Zhou, "CrowdCLIP: Unsupervised crowd counting via vision-language model," in *Proc. CVPR*, Vancouver, BC, Canada, 2023, pp. 10231–10240, doi: 10.1109/CVPR52723.2023.00986.

[21] J. Wan, S. Ma, J. Lin, and A. J. Ma, "Robust zero-shot crowd counting and localization with adaptive resolution SAM," in *Proc. ECCV*, Milan, Italy, 2024, pp. 1–18.

[22] H. Lin, Z. Ma, R. Ji, Y. Wang, Z. Su, X. Hong, and D. Meng, "Semi-supervised counting via pixel-by-pixel density distribution modelling," *IEEE Trans. Pattern Anal. Mach. Intell.*, vol. 47, no. 1, pp. 1–14, 2025, doi: 10.1109/TPAMI.2024.3435198.

[23] Y. Liu, Z. Wang, M. Shi, S. Satoh, Q. Zhao, and H. Yang, "Towards unsupervised crowd counting via regression-detection bi-knowledge transfer," in *Proc. ACM MM*, Seattle, WA, USA, 2020, pp. 129–137, doi: 10.1145/3394171.3413556.

[24] J. Cheng, Q. Li, J. Chen, and M. Gao, "Crowd counting via lightweight neural networks: a literature review," *Meas. Sci. Technol.*, vol. 36, no. 7, Art. no. 072001, 2025, doi: 10.1088/1361-6501/ad39cc.

[25] X. Guo, K. Song, M. Gao, W. Zhai, Q. Li, and G. Jeon, "Crowd counting in smart city via lightweight ghost attention pyramid network," *Future Gener. Comput. Syst.*, vol. 147, pp. 328–338, 2023, doi: 10.1016/j.future.2023.05.013.

[26] Y. Liu, G. Cao, H. Shi, and Y. Hu, "LW-Count: An effective lightweight encoding-decoding crowd counting network," *IEEE Trans. Circuits Syst. Video Technol.*, vol. 32, no. 10, pp. 6821–6834, 2022, doi: 10.1109/TCSVT.2022.3175604.

[27] Z. Shen, G. Li, R. Xia, H. Meng, and Z. Huang, "A lightweight object counting network based on density map knowledge distillation," *IEEE Trans. Circuits Syst. Video Technol.*, vol. 35, no. 2, pp. 1492–1505, 2024, doi: 10.1109/TCSVT.2024.3414578.

[28] J. Yi, F. Chen, Z. Shen, Y. Xiang, S. Xiao, and W. Zhou, "An effective lightweight crowd counting method based on an encoder-decoder network for the internet of video things," *IEEE Internet Things J.*, vol. 11, no. 2, pp. 3082–3094, 2023, doi: 10.1109/JIOT.2023.3302340.

[29] H. Lee and J. Lee, "TinyCount: An efficient crowd counting network for intelligent surveillance," *J. Real-Time Image Process.*, vol. 21, no. 1, Art. no. 153, 2024, doi: 10.1007/s11554-024-01440-3.

[30] K. Wu, J. Zhang, H. Peng, M. Liu, B. Xiao, J. Fu, and L. Yuan, "TinyViT: Fast pretraining distillation for small Vision Transformers," in *Proc. ECCV*, Tel Aviv, Israel, 2022, pp. 627–644, doi: 10.1007/978-3-031-19799-1_37.

[31] H. Idrees, M. Tayyab, K. Athrey, D. Zhang, S. Al-Maadeed, N. Rajpoot, and M. Shah, "Composition loss for counting, density map estimation and localization in dense crowds," in *Proc. ECCV*, Munich, Germany, 2018, pp. 532–546, doi: 10.1007/978-3-030-01216-8_33.

[32] Q. Wang, J. Gao, W. Lin, and X. Li, "NWPU-Crowd: A large-scale benchmark for crowd counting and localization," *IEEE Trans. Pattern Anal. Mach. Intell.*, vol. 43, no. 6, pp. 2141–2149, 2020, doi: 10.1109/TPAMI.2020.2992459.

[33] Q. Wang, J. Gao, W. Lin, and Y. Yuan, "Pixel-wise crowd understanding via synthetic data," *Int. J. Comput. Vis.*, vol. 129, no. 1, pp. 225–245, 2021, doi: 10.1007/s11263-020-01367-y.

[34] X. Guo, M. Gao, W. Zhai, Q. Li, and G. Jeon, "Scale region recognition network for object counting in intelligent transportation system," *IEEE Trans. Intell. Transp. Syst.*, vol. 24, no. 12, pp. 15920–15929, 2023, doi: 10.1109/TITS.2023.3292415.

[35] W. Zhai, X. Xing, and G. Jeon, "Region-aware quantum network for crowd counting," *IEEE Trans. Consum. Electron.*, vol. 70, no. 1, pp. 5536–5544, 2024, doi: 10.1109/TCE.2024.3364972.

[36] J. Wang, X. Guo, Q. Li, A. M. Abdelmoniem, and M. Gao, "SDAnet: Scale-deformation awareness network for crowd counting," *Proc. IEEE*, vol. 112, no. 5, Art. no. 043002, 2024, doi: 10.1109/JPROC.2024.3381254.

[37] M. Xi and H. Yan, "Lightweight multi-scale network with attention for accurate and efficient crowd counting," *Vis. Comput.*, vol. 40, no. 7, pp. 4553–4566, 2024, doi: 10.1007/s00371-023-03043-4.

[38] J. Yi, Z. Shen, F. Chen, Y. Zhao, S. Xiao, and W. Zhou, "A lightweight multiscale feature fusion network for remote sensing object counting," *IEEE Trans. Geosci. Remote Sens.*, vol. 61, pp. 1–13, Art. no. 5621413, 2023, doi: 10.1109/TGRS.2023.3312487.

[39] L. Liang, H. Zhao, F. Zhou, M. Ma, F. Yao, and X. Ji, "PDDNet: Lightweight congested crowd counting via pyramid depth-wise dilated convolution," *Appl. Intell.*, vol. 53, no. 9, pp. 10472–10484, 2023, doi: 10.1007/s10489-022-03991-8.

[40] C. Lin and X. Hu, "Efficient crowd density estimation with edge intelligence via structural reparameterization and knowledge transfer," *Appl. Soft Comput.*, vol. 154, Art. no. 111366, 2024, doi: 10.1016/j.asoc.2024.111366.

[41] J.-a. Cheng, Q. Li, A. Souri, X. Lei, C. Zhang, and M. Gao, "Towards trustworthy crowd counting by distillation hierarchical mixture of experts for edge-based cluster computing," *Cluster Comput.*, vol. 28, no. 7, 2025, doi: 10.1007/s10586-025-05226-y.

[42] H. Lin, Z. Ma, X. Hong, Y. Wang, and Z. Su, "Semi-supervised crowd counting via density agency," in *Proc. ACM MM*, Lisbon, Portugal, 2022, pp. 1416–1426, doi: 10.1145/3503161.3548366.

[43] W. Lin and A. B. Chan, "Optimal transport minimization: crowd localization on density maps for semi-supervised counting," in *Proc. CVPR*, Vancouver, BC, Canada, 2023, pp. 21663–21673, doi: 10.1109/CVPR52723.2023.02074.

[44] X. Wei, Y. Qiu, Z. Ma, X. Hong, and Y. Gong, "Semi-supervised crowd counting via multiple representation learning," *IEEE Trans. Image Process.*, vol. 32, pp. 5220–5230, 2023, doi: 10.1109/TIP.2023.3313490.

[45] S. Zhang, Y. Wang, Q. Li, and M. Gao, "Boosting semi-supervised crowd counting with scale-based active learning," in *Proc. ACM MM*, Melbourne, VIC, Australia, 2024, pp. 3542–3551, doi: 10.1145/3664647.3680879.